

Facile synthesis of silver nanoparticles for antibacterial application against multidrug resistant bacteria and antioxidant activity

Sonia Tyagi¹, Pamela Singh^{1*}, Vipin Khasa²

¹Department of Biotechnology, Deenbandhu Chhotu Ram University of Science and Technology, Mурthal, Sonipat, Haryana, India

²Department of Animal Husbandry, Sonipat, Haryana, India

***Corresponding author :**

Dr. Pamela Singh

Department of Biotechnology, Deenbandhu Chhotu Ram University of Science and Technology, Mурthal, Sonipat-131039, Haryana, India

Email ID : pamelasingh.bt@dcrustm.org

DOI: <https://doi.org/10.64149/J.Carcinog.22.2.166-179>

ABSTRACT

The current study investigated the optimization of physicochemical parameters for the phyto-synthesis of silver nanoparticles (AgNPs) using aqueous extracts from *Hibiscus rosa sinensis* leaves. The study examined the effects of various factors, including reaction time, temperature, silver nitrate concentration, plant extract volume, and pH on the synthesis of AgNPs. Spectrophotometric analysis indicated optimal conditions for AgNP synthesis at a silver nitrate concentration of 4 mM, a plant extract ratio of 2:8, a temperature of 55 °C, and a pH of 13, resulting in a peak absorption at 419 nm. Fourier Transform Infrared (FTIR) spectroscopy identified the presence of functional groups responsible for capping and stabilizing the AgNPs, while Zeta potential measurements indicated a net surface charge of -29 mV, suggesting stability against agglomeration. X-ray Diffraction (XRD) analysis confirmed the crystalline nature of the synthesized AgNPs, with an estimated particle size of 23.3 nm. The antibacterial activity of the AgNPs was evaluated, showing significant inhibition against various multi drug resistant pathogenic bacteria, with the highest activity against *S. flexneri* and *E. coli*. Additionally, the synthesized AgNPs exhibited notable antioxidant activity, demonstrating their potential as therapeutic agents. Overall, this study emphasizes the significance of optimizing synthesis conditions for enhancing the properties of AgNPs and their applicability in biomedical fields.

Keywords: Silver nanoparticles, *Hibiscus rosa sinensis*, antioxidant, antibacterial, FTIR, XRD

How to Cite: Sonia Tyagi, Pamela Singh, Vipin Khasa, (2023) Facile synthesis of silver nanoparticles for antibacterial application against multidrug resistant bacteria and antioxidant activity, *Journal of Carcinogenesis*, Vol.22, No.2, 166-179

1. INTRODUCTION

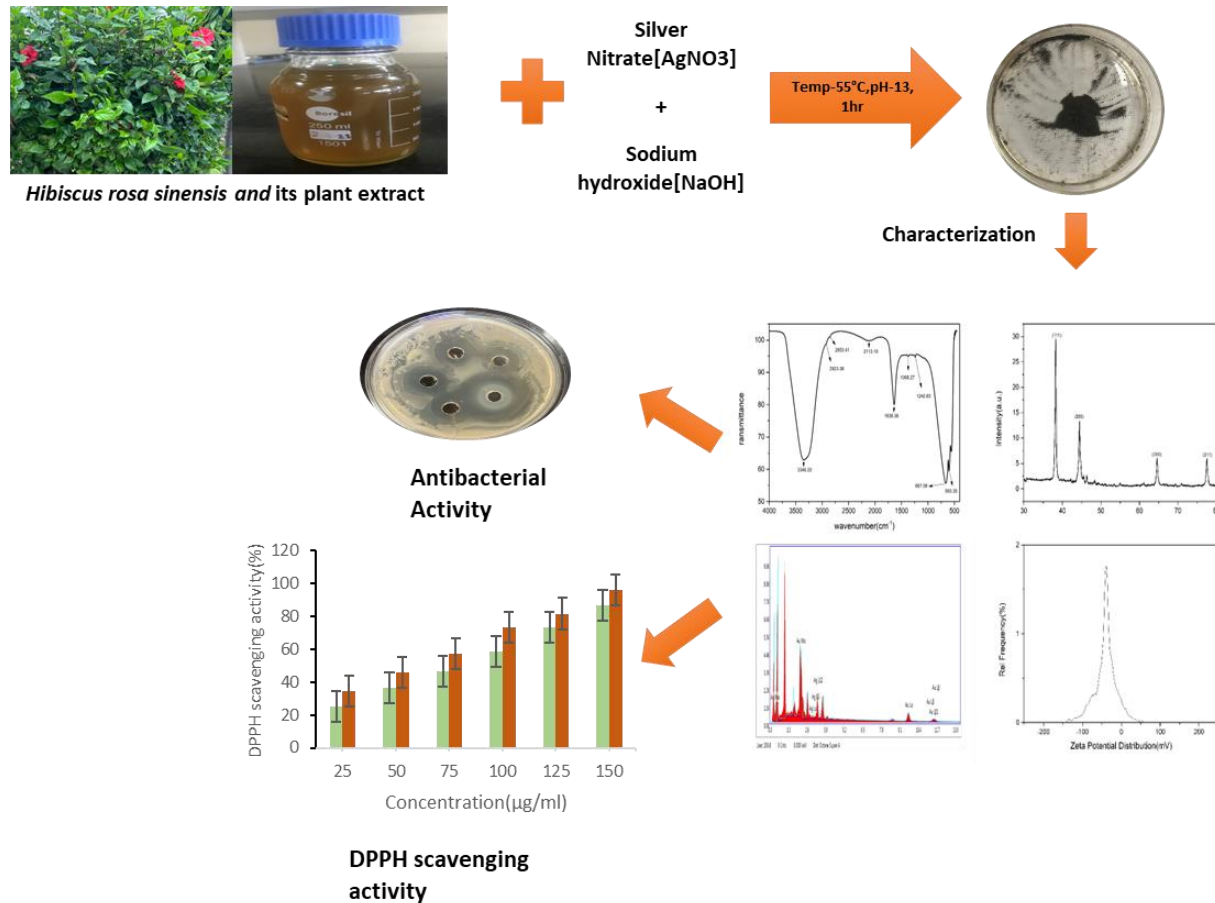
Nowadays, nanoscience is a prominent field of study that offers opportunities for fundamental and experimental study in all areas of cognitive science. A global technological revolution is being propelled by the emergence of nanoscience and nanotechnology[1]. Nonetheless, creating nanoparticles (NPs) with the appropriate quality is a crucial component of modern nanotechnological methods. Numerous studies detailing various techniques for synthesizing metal NPs involving reductions carried out by chemical, electrochemical, photochemical, and other means have been published[2-4]. However, it has been reported that biological approaches outperform chemical ones in regards to environmental safety and economic viability. The deliberate exploitation of microorganisms for the biosynthesis of AgNPs has recently emerged[5]. Although it has achieved a degree of success, but the use of plant-based materials as opposed to microorganisms for the environmentally friendly synthesis of metal NPs has drawn a lot of attention due to their lower toxicity, shorter processing times, and the added benefit of readily available natural capping agents. Additionally, it uses a variety of reductant sources, including leaves, flowers, and catkins, and also minimizes the cost of isolating microorganisms and improving culture conditions for microbe-assisted biosynthesis[6-11].

Although the precise mechanism by which AgNPs combat fearsome diseases is unknown but researchers have postulated various mechanisms in light of their findings. The positive charge of silver ions facilitates their interaction with negatively charged cellular components, leading to cell membrane disruption, ROS generation, and DNA damage[12]. The other characteristics of Ag⁺ include their capacity to engage with the thiol group (-SH group) of enzyme active sites, forming the

stable complex Ag-S, and obstructing an enzyme's active site, which causes cells to succumb from inadequate respiration[13,14]. This multi-faceted mechanism is why AgNPs are effective against a broad range of microorganisms.

Besides, AgNPs are also reported for their diverse biological applications, particularly their antibacterial, anti-biofilm, and antiviral properties[15-19]. An alternative to the chemical agents has become essential for the management of infections in medicine and various other industries. The colloidal silver has emerged as a modern standard in hospital intensive care units for the preventive treatment of ventilator-acquired pneumonia. AgNPs are effective and appropriate antibacterial agents, either used alone or in conjunction with currently available antibiotics[20-22]. Pharmacologically significant compounds that might possess potential in therapeutics could be retained during bioreduction by the biosynthesized AgNPs[23].

Graphical abstract



Highlights

- Fabrication of AgNPs using *Hibiscus rosa sinensis* for reduction and stabilization.
- Physicochemical characterization of synthesized AgNPs using FTIR, XRD, Zeta Potential, TEM, SEM and EDX.
- Antimicrobial Profiling of synthesized AgNPs against the pathogenic bacteria.

Antioxidant potential of synthesized AgNPs using DPPH assay

There have been reports of the synthesis of AgNPs utilizing a variety of plants, including *Cucumis prophetarum*, *Azadirachta indica*, *Myrmecodia pendans*, *Rhynchosciadium ellipticum*, and waste tea leaves[24-28]. The exceptional sizes of different nanometer scales of AgNPs are provided by each plant extract. One such medicinal plant whose extract is utilized in the fabrication of AgNPs is *H. rosa sinensis*.

Hibiscus being an ornamental plant traditionally used as aphrodisiac, demulcent, emollient, laxative, anodyne, refrigerant and has anti-inflammatory properties. The phytochemicals found in this plant have therapeutic value, including tannins, carotene, thiamine, riboflavin, niacin, anthocyanin pigment, flavonoids, and ascorbic acid[29]. Antitumor, antidiarrheal, antiestrogenic, antispermatic, androgenic, antiphlogistic, wound healing, and anticonvulsant are merely a few of its other therapeutic properties[30].

To the best of our knowledge, there have been relatively few investigations on the biosynthesis of AgNPs utilizing *H. rosa*

sinensis leaf extract, and a significant research gap has been identified. The purpose of this work is to employ *H.rosa sinensis* leaf extract in an inexpensive and environmentally friendly method for producing AgNPs in a biogenic manner.

2. EXPERIMENTAL SECTION:

2.1 Extraction of *H.rosa sinensis* plant extract and Bio-fabrication of AgNPs

The *H.rosa sinensis* leaves were collected from campus nursery of Deenbandhu Chhotu Ram university of Science and Technology, Murthal. The preparation of plant aqueous extract was done by heating plant powder in distilled water (1:10 ratio respectively) for 30 min and was filtered. to separate the plant's aqueous extract from the powder using syringe filters [31,32].

The aqueous plant extract was used to reduce 1mM of silver nitrate in a 1:9 ratio respectively. The reaction mixture was agitated continuously while its temperature was kept at 60°C at pH 9. Absorbance of light for an aliquot from the reaction mixture was measured used to monitor the synthesis of the AgNPs by UV-Vis spectrophotometer (UV-3092 , Labindia Analytical Instruments Pvt. Ltd) within the range of 200-700nm. Upon completion of the synthesis, the AgNPs were extracted from the colloidal mixture using centrifugations at 1000×g thrice with distilled water and final washing was done with 95% ethanol to stop the reaction further[12].

2.3 Optimization of synthesis parameters of AgNPs

The volume of plant extract, pH, temperature, reaction time, and metal salt volume are some of the variables that affect the green synthesis of NPs[33].

UV-Visible spectroscopy of the nanosuspension was carried out at various time intervals viz. 0.5h, 1h, 2h, and 24h. The experiment was set up in an incubator for one hour in order to examine the effects of different temperatures (25°C, 35°C, 45°C, 55°C, 65 °C). Thereafter, each solution was exposed to a UV spectrophotometer operating between 200 and 800 nm in order to observe the spectra. Numerous concentrations of silver nitrate—namely, 1mM, 2mM, 3mM, and 4mM—were employed to optimize the substrate concentration for the fabrication of AgNPs. The ratios of variable plant extract to silver nitrate i.e. 1:9, 2:8, 3:7, 4:6, and 5:5 were also investigated. A range of pH values (7,9,11 and 13) were taken into consideration while synthesizing AgNPs. The synthesis of silver NPs was confirmed by observing a color change in the solutions after the completion of the reaction and was assessed using UV-Vis spectrophotometer.

2.4 Physical and optical characterization of synthesized AgNPs

A variety of material characterization techniques were used to assess the synthesized AgNPs under optimal conditions both optically and morphologically.

The organic functional groups affixed to the surface of AgNPs were investigated using Fourier transform infrared spectroscopy (FTIR) in the 4000-500cm⁻¹ range were obtained using Perkin Elmer's FT-IR Spectrophotometer Frontier equipped with the Attenuated Total Reflectance (ATR) accessory. The surface charge potentiality of the synthesized NPs was measured in order to figure out their stability using an Anton Paar Particle Analyzer Lite Sizer 500. The analysis was conducted at a temperature of 25°C, and the result was noted as an operation of time. The dried sample was then put through XRD analysis in order to assess the crystallinity and purity of synthesized AgNPs using an X-ray wavelength of 1.5406, the Ultima IV (Rigaku, Japan) was used to generate an XRD scan in the 20-70 degree range and was conducted consistently with a step size of 0.02 and a speed of 2 degrees per minute. The morphology of synthesized particles at the submicron scale and elemental information at the micron scale were analyzed using scanning electron microscopy (SEM)(ZEISS EVO 18). Utilizing energy-dispersive X-ray spectroscopy, the elemental makeup of synthesized AgNPs was investigated with EDX spectroscopy(EDX-AMETEK).The size and shape of the particles were assessed using transmission electron microscope (THERMO SCIENTIFIC TELOS) operating at an accelerating voltage of 200 kV.

2.5 Biological applications

2.5.1 Antioxidant activity of synthesized AgNPs

The antioxidant potential of AgNPs was quantitatively investigated with the use of the in-vitro 2,2-diphenyl-1-picrylhydrazyl (DPPH) assay [34]. Using L-ascorbic acid as a control standard solution and DPPH as a blank solution, 1 ml of DPPH solution was mixed to 1 ml of standard and test NPs at varying concentrations. Samples were prepared using 50% methanol as solvent. The absorbance at 517 nm was measured after the test sample was incubated for 30 min at room temperature in the dark. The percentage of radical scavenging activity was computed using

$$\%RSA = A_c - A_t/A_c \times 100$$

where A_c and A_t denote absorbance of blank DPPH solution and test samples (AgNPs added to DPPH solution), respectively.

2.5.2 Antibacterial evaluation of synthesized AgNPs

Mannitol salt agar (MSA) medium was used to test the antibacterial effectiveness of AgNPs against pathogenic bacteria, including *Escherichia coli*, *Shigella flexneri*, *Staphylococcus aureus*, and *Klebsiella pneumonia*, which were available in the laboratory at the Department of Biotechnology, DCRUST, Murthal. Wells were bored after inoculation of 0.5 mL of pathogenic culture on MHA medium plates. The synthesized AgNPs were added to each well at a varying concentration (10 to 90 μ g/mL). The plates were subsequently incubated in upright position at 37°C for 24hrs. The diameter of zone of inhibition (ZOI) was measured in millimeters (mm), demonstrating the potential of AgNPs to impede the proliferation of bacteria.

2.5.3 MIC and MBC of synthesized AgNPs

The bacterial growth in serially diluted NP suspensions was examined in order to determine the MIC value. 2ml of broth was transferred into sterile tubes, and the first tube was then utilized for the 2-fold dilution of tubes with consecutive numbers after adding 2ml of AgNPs (256 μ g/mL). Following the addition of 50 μ L of bacterial culture suspension, the tubes were incubated at 37 °C for 24hrs. The presence or absence of bacterial growth was confirmed visually and MIC values were obtained by spectrophotometer readings at 600 nm. The bacterial growth was then measured and the minimum bactericidal concentration (MBC) was determined by pouring the mixture onto a nutrient agar plate[35].

2.8 Data processing

The reproducibility of the experiments conducted was confirmed on performing them in a triplicate arrangement and the data were reported as mean \pm standard deviation. The absorbance spectrum of the NPs was re-plotted using Originpro9. A one-way analysis of variance (ANOVA) was performed to evaluate the statistical significance of the antibacterial activity of the NPs, with a p-value of less than 0.05 ($P < 0.05$) considered indicative of a statistically significant difference.

3. RESULTS AND DISCUSSION

3.1 Optimization of the Phyto-synthesis of AgNPs

With an increase in time from 0.5 to 3 hours, an increase in absorbance of the peak were observed. The time taken to induce a color change in the reaction mixture is a reflection of the interaction between the phytochemicals in the plant extract and the metal ions[36]. The optimum synthesis of AgNPs has been documented after 25 minute incubation period using *Rosa damascena* leaf extracts[37]. However, in the current study, the spectrum did not get stabilize and the sharp absorbance peak at 426nm was observed after 1 hour of incubation for the AgNPs synthesized utilizing *H.rosa sinensis* (fig. 1a). However, the highly intense peak was even observed after 24 hrs of incubation . But this is explained by the theory reported earlier that extended reaction time can result in more significant particle growth and increased aggregation, and can also lead to changes in the crystal structure affecting the potential and stability of NPs[38,39].

An increase in the absorbance of the resulting suspension was observed when the temperature was increased from 25 °C to 65 °C. Significantly broader and less intense peaks were observed at lower temperatures, indicating inefficient AgNPs synthesis. There was a steady increase in absorption and sharpening of peak with increasing temperature. We, hereby, report 55 °C as the optimum temperature for synthesis of particles using *H.rosa sinensis* leaf extract(fig. 1b). Qasim et al[40] and Ansari et al[41] reported similar results using extracts of *Seriphidium quettense* and *Azadirachta indica*, respectively, and found that higher temperatures were more appropriate for the synthesis of small-sized NPs.

The absorbance was increased with the increase in the concentration of silver nitrate from 0.5 to 3mM and an intense peak was observed. An intense peak was observed at 416nm when the concentration was increased to 4mM for AgNPs synthesized with *H. rosa sinensis* leaf extract(fig.1c). The findings were found to be consistent with those published by other researchers[42-44]. Furthermore, Ansari et al[41] have reported that larger and more aggregated NPs are formed on increasing the concentration of silver nitrate.

The observation of an intense and sharp peak at 449nm in the UV-Vis spectra when using a concentration ratio of 2:8(fig.1d) indicating optimum volume of plant extract . After that, there was a noticeable peak broadening and a decrease in absorbance when the ratio of leaf extract increased in the reaction mixture. According to Jalab et al[45], increasing the amount of extract in the reaction mixture increased the absorbance of the nanoparticle suspension while synthesizing AgNPs from *Acacia cyanophylla* extract.

The intense peak for the synthesized AgNPs with the aid of *H. rosa sinensis* leaf extract was observed at 423nm at pH 13(1e). Similar trends have been reported earlier by [46] while synthesizing AgNPs using Rudanti fruit extract, where increasing the reaction mixture pH, increased the peak intensity and rate of nanoparticle formation. When the pH is alkaline, the clusters are entirely charged, maximizing the repulsive electrostatic/electrosteric interactions, which increases the stability of the cluster dispersion and colloid formation while decreasing the tendency for the particles to aggregate[39,46].

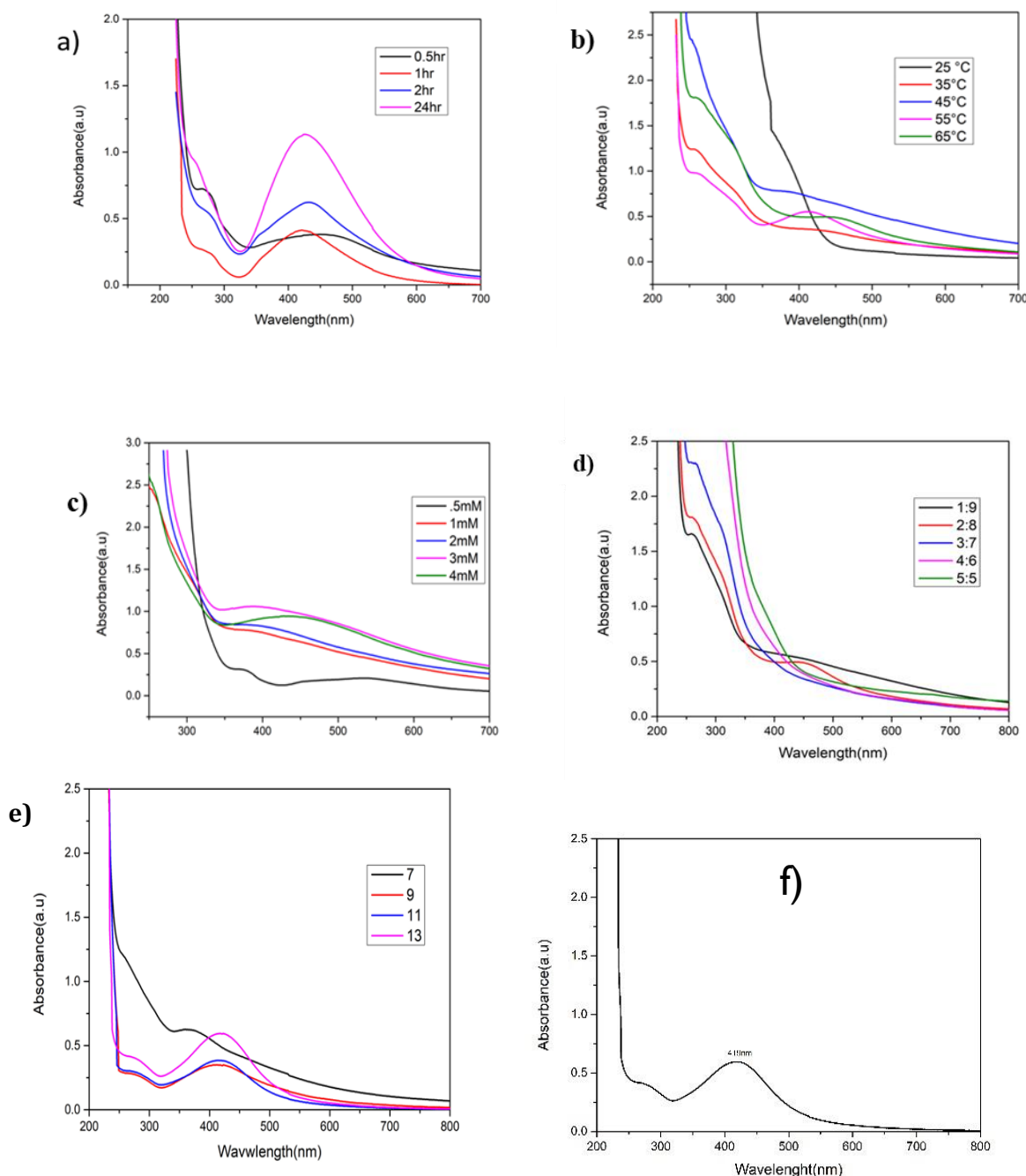


Fig1: Optimization of synthesis parameters for AgNPs synthesis: a) Effect of metal ion concentration; b) effect of plant leaf extract volume; c) Effect of pH; d) effect of temperature; e)effect of time; f) UV-Vis spectra of synthesized AgNPs

3.2 Synthesis of AgNPs under the optimized conditions

The spectrophotometric data demonstrated that the optimal synthesis of AgNPs was achieved by mixing 4 mM AgNO₃ with the plant extract in a 8:2 ratio, respectively, at 55 °C and 13 pH (fig. 1f)(Table 1). The highest peak in the UV-visible spectrum, which is indicative of the synthesis of AgNPs, was seen at 419 nm. *Mimosa pigra* [47], *Ginkgo biloba* [48] and *Lantana trifolia* [49] were the subjects of several earlier investigations on the influence of various physicochemical parameters on the synthesis of NPs. The outcomes of these investigations corroborate our conclusions that physicochemical factors can be adjusted to customize the size and form of NPs under ideal reaction circumstances.

Table1: Optimized parameters for synthesized AgNPs

Parameters	Optimized value
Silver nitrate Concentration	4mM
Plant Extract Volume	2:8
Temperature	55°C
Time	1hr
pH	13

3.3 Physical and optical characterization of synthesized AgNPs

The FTIR spectrum of synthesized AgNPs showed absorption bands at 3346.20, 2923.38, 2853.41, 2113.10, 1638.36, 1368.27, 1242.63, 667.08 & 593.35 cm^{-1} (Table 2)(fig. 2). The peaks at 2923.38 cm^{-1} and 2853.41 cm^{-1} are assigned to the stretching vibrations of CH_2 and CH_3 groups, while the band at 3346.20 cm^{-1} is indicative of the $-\text{OH}$ stretching vibration [43,50]. The bands at 1638.36 cm^{-1} represented carbonyl stretch ($-\text{C=O}$) in proteins[51].The peaks at approximately 667.08 and 593.35 cm^{-1} corresponded to C-H bonds of alkenes and (C-Cl) stretching of the alkyl halides bond respectively [52,53,51]. According to the FTIR analysis, proteins or amino acids are still adhering to the AgNP surface in a proximity-based manner could function as a barrier to stearic or electrostatic attraction and inhibit AgNPs aggregation[54,55]. In support of the earlier research, it has been demonstrated that the protein component of plant extracts contributes to the reduction and capping of NPs [56].

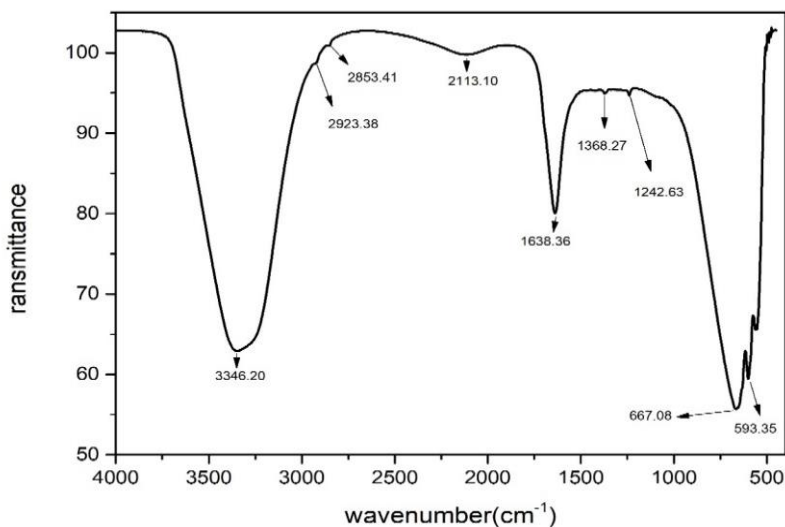


Fig 2: FTIR spectrum of synthesized AgNPs

Table 2: FTIR bands and functional groups of synthesized AgNPs

Wavenumber, cm^{-1}	Functional group
3346.20	H bonded $-\text{OH}$ group stretch, $-\text{NH}_2$ group stretching
2923.38 & 2853.41	stretching vibrations of CH_2 and CH_3 groups
2113.10	$-\text{C}\equiv\text{C}-$ stretch of alkynes
1638.36	carbonyl stretch ($-\text{C}=\text{O}$) in proteins
1368.27	C-N stretching of aromatic amines
1242.63	($-\text{CH}_2\text{X}$) of alkyl halides,
667.08	C-H bonds of alkenes
593.35	(C-Cl) stretching of the alkyl halides bond

With a net surface charge of -29 mV (fig. 3a), the synthesized NPs were shown to be relatively durable and to have a low propensity to agglomerate. Zeta potential values with dimensions <-30 and $>+30$ are considered highly stable, with less likelihood of forming agglomerations because of a higher probability of interparticle repulsion [57].

Significant peaks at 2θ values of 38.22° , 44.44° , 64.53° , and 77.51° were observed in the XRD pattern; coincided with those listed in the Silver JCPDS file, 04-0783. Based on peak indexing and data analysis, the 2 values for FCC structures attributed to (111), (200), (220), and (311) planes of Bragg's reflections (Table 3). Particle size was computed using OriginPro 9.0. The particle size was determined to be 23.3 nm which falls in the range of TEM analysis.

Table 3: XRD peak indexing and d-spacing

Peak 2θ	θ	$\sin \theta$	d (nm)	hkl
38.22	19.11	0.257	0.299	111
44.44	22.22	0.226	0.340	200
64.53	32.26	0.747	0.103	220
77.51	38.75	0.872	0.088	311

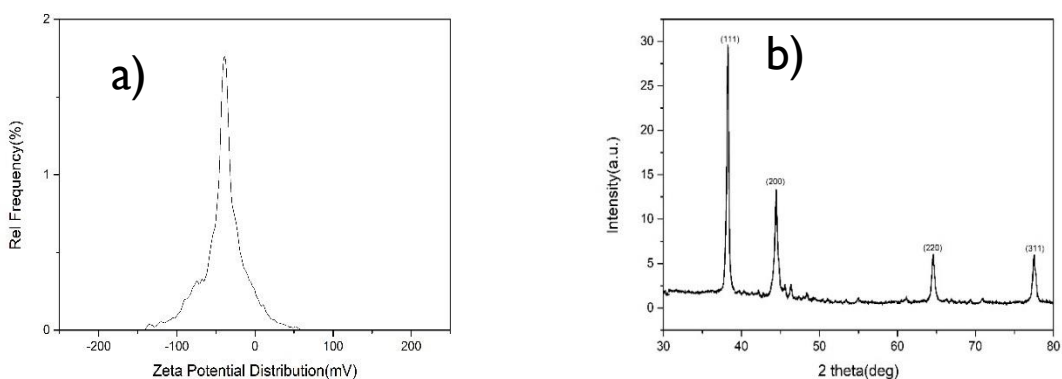


Fig. 3: a) Zeta potential of synthesized AgNPs; b) X-ray diffraction for synthesized AgNPs

The synthesized AgNPs were quasi spherical in shape shown in SEM image (fig. 4a). The elemental composition of the 10.50% Au and 89.50% Ag found in the EDX evaluation verified the pure nature of the NPs produced (fig. 4c). Au was detected since it was used as the coating material for the EDX study. Additional investigations have demonstrated that

AgNPs share a similar elemental composition [12].

AgNPs synthesized from *H. rosa sinensis* leaf extract were shown to have an uneven size distribution, ranging from 7 to 80 nm as depicted in TEM image (fig. 4a). Comparable patterns have also been shown in the synthesis of AgNPs employing leaf extract from *Elettaria cardamomum*, where NPs with the 5-80 nm size range were discovered [56].

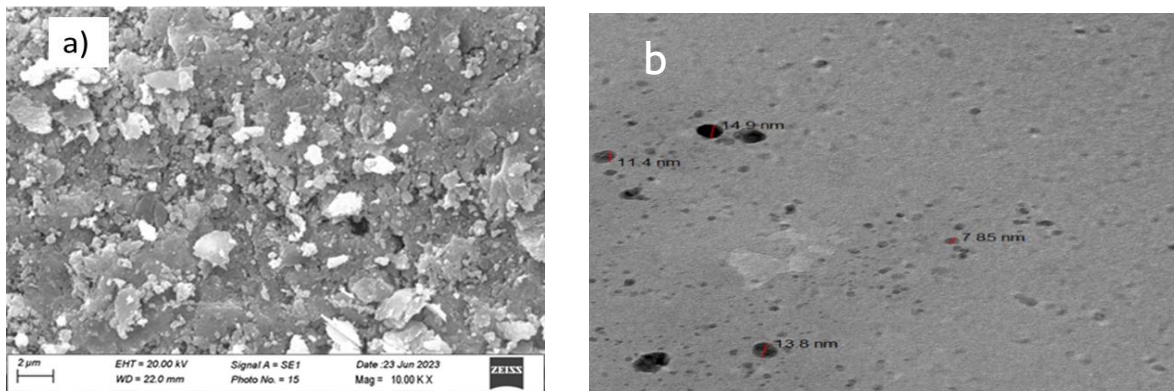
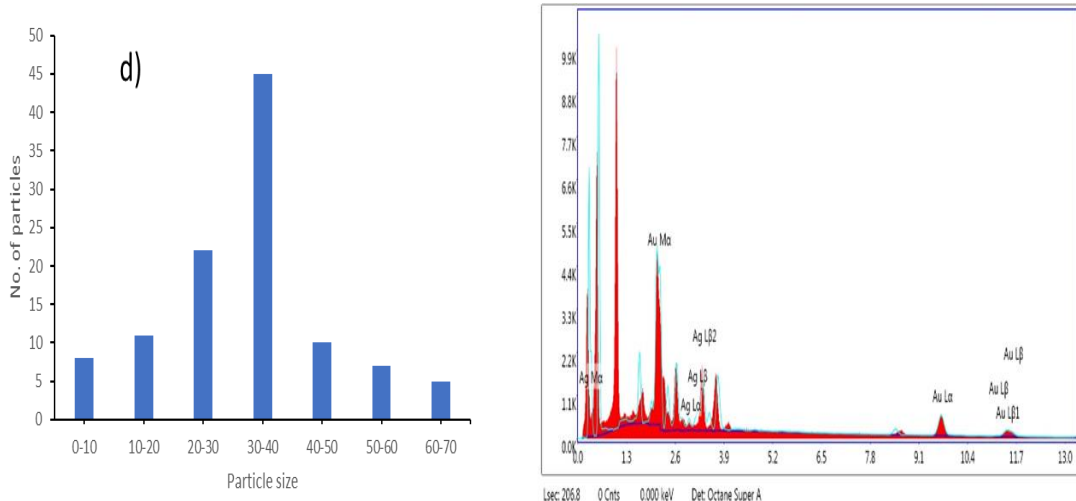


Fig. 4: a)SEM ;b) TEM ; c) EDX image of synthesized AgNPs; and d) Particle size distribution



3.4 Biological applications

3.4.1 Antioxidant activity of synthesized AgNPs

Stable free radical DPPH, purple in color, has a noticeable absorption maximum at 517 nm. Antioxidants counteract the free radical in DPPH, lowering absorbance and color intensity. The amount of DPPH radicals is decreased by Ag-NPs' propensity to donate protons or electrons [58]. Fig. 5 illustrates DPPH scavenging activity of AgNPs. The indication of radical scavenging activity include a reduction in the absorbance of the parent DPPH solution with increasing nanoparticle concentration. AgNPs were just as effective as the control, demonstrating 86.23% radical scavenging at a high concentration of 150 μ g/mL. The IC50 was computed to be 84.03 μ g/ml.

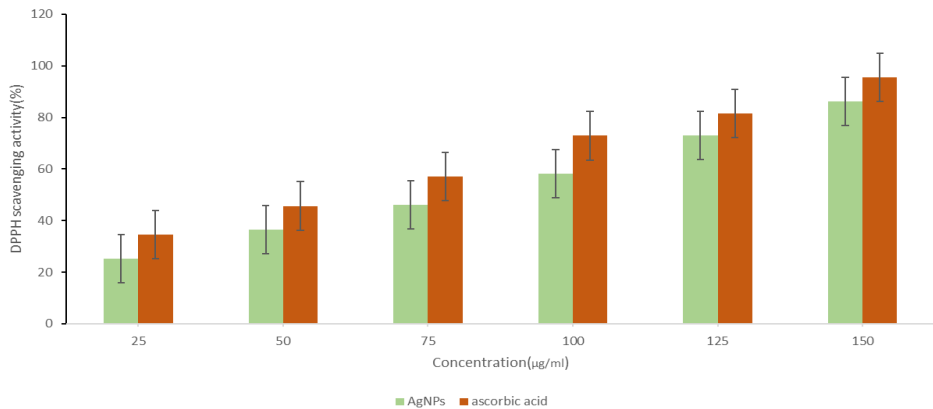


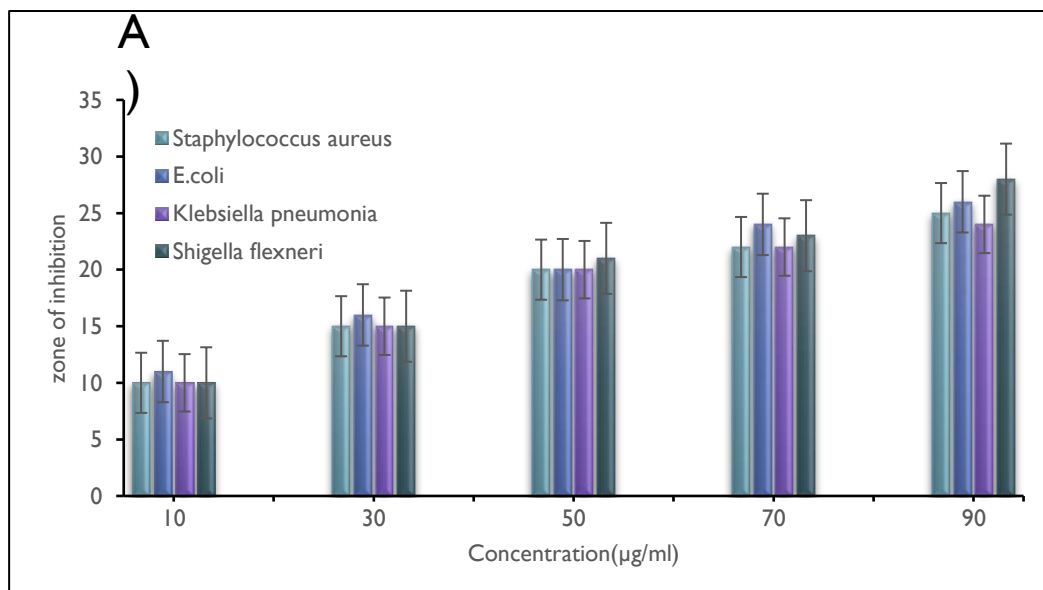
Fig. 5: DPPH radical scavenging activity of AgNPs and ascorbic acid

3.4.2 Antibacterial evaluation of synthesized AgNPs

The findings of the antimicrobial evaluation are summarized in Table 4. AgNPs showed variance in ZOI, with diameters ranging from 10 to 28 mm, as evident from the data(fig. 6A). Table 4 clearly illustrates that increasing the concentration of NPs from 10 to 90 μ L, increased the antibacterial activity of pathogenic bacteria. The highest antibacterial activity was shown against *S. flexneri*, *E.coli*, *S.aureus* followed by *K. pneumonia* with 90 μ g/ml inhibitory concentration(fig.6B). Conclusively, it was found that the synthesized AgNPs possessed strong antibacterial potential against the pathogenic microorganisms. This was attributed to the fact that the multiple mechanism of actions of NPs i.e. disruption of cell membrane and cell wall, denaturation of proteins, impairs the electrolyte balance and generation of reactive oxygen species simultaneously against the pathogenic bacteria could possibly make them a potential therapeutic agent[59].

3.5 MIC and MBC of synthesized AgNPs

The MIC study was performed to evaluate the growth of bacteria while increasing NP dilutions. The growth pattern at 600 nm was documented in addition to a visual examination of the outcomes. The MIC and MBC values of AgNPs were determined for each pathogenic bacterium. A significant value of MIC was observed for *E.coli*(112 μ g/ml).The MIC value for *K. pneumonia*, *S. flexneri* and *S. aureus* was observed to be 87, 83, and 82 respectively(Table 5).The synthesized AgNPs were found to have strong antibacterial action against the pathogens under investigation, as indicated by the estimated value for $p \leq 0.05$.



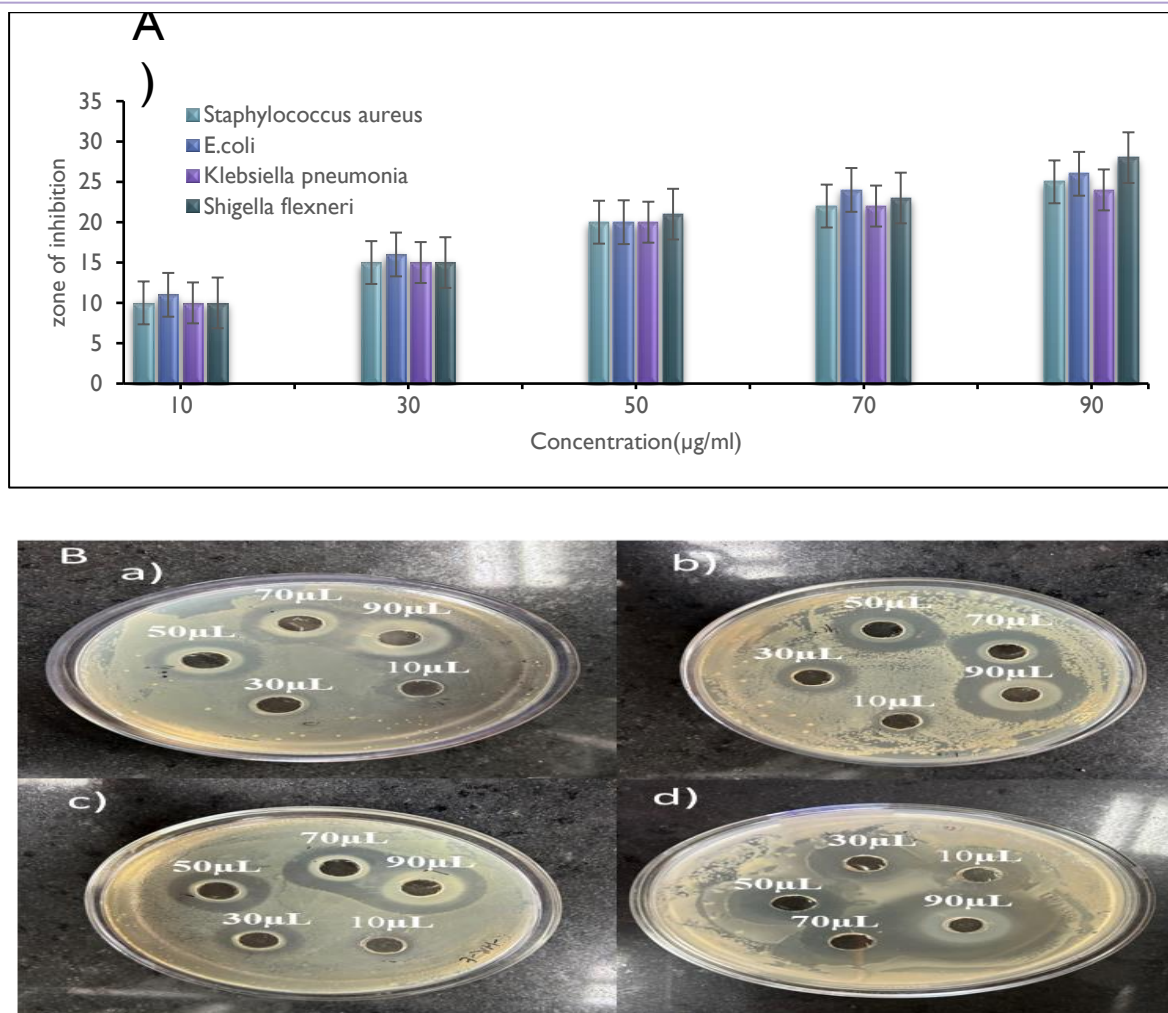


Fig.6 A) Comparative inhibition zones of AgNPs against distinct bacteria ;**B)** Inhibition zones against a) *S.aureus*, b) *E.coli*, c) *Klebsiella pneumonia*, d) *Shigella flexneri*

Table4: Antibacterial ability of the synthesized AgNPs against pathogenic microorganisms

S.no.	Bacterial pathogen	Zone of inhibition(mm \pm SD)				
		10 $\mu\text{g/ml}$	30 $\mu\text{g/ml}$	50 $\mu\text{g/ml}$	70 $\mu\text{g/ml}$	90 $\mu\text{g/ml}$
1	<i>Staphylococcus aureus</i>	10 \pm 0.4	15 \pm 0.1	20 \pm 0.04	22 \pm 0.2	25 \pm 0.4
2	<i>Escherichia coli</i>	11 \pm 0.1	16 \pm 0.2	20 \pm 0.2	24 \pm 0.1	26 \pm 0.3
3	<i>Klebsiella pneumonia</i>	10 \pm 0.2	15 \pm 0.2	20 \pm 0.1	22 \pm 0.4	24 \pm 0.02
4	<i>Shigella flexneri</i>	10 \pm 0.5	15 \pm 0.4	21 \pm 0.2	23 \pm 0.2	28 \pm 0.3

Table5: MIC/MBC of AgNPs against pathogenic microorganisms

Bacterial pathogens	MIC(µg/ml)	MBC(µg/ml)
<i>Staphylococcus aureus</i>	82	76
<i>E.coli</i>	112	110
<i>Klebsiella pneumonia</i>	87	81
<i>Shigella flexneri</i>	83	78

4. CONCLUSION

The aforementioned study verify the application of *H.rosa sinensis* leaf aqueous extracts for environmental friendly one-pot synthesis of AgNPs and their usage as biological control agents against pathogenic bacterial strains. The morphological characterization of AgNPs indicated that they are mostly in the range of about 7-80 nm, while the particle size analysis from XRD data revealed that they occur in the size range of around 23.3 nm which is in agreement with the particle size revealed by TEM analysis. The utilization of plant-derived AgNPs to biologically regulate the growth of pathogenic bacterial strains is strongly supported by our findings. Numerous studies have been conducted on the production of NPs using *H. rosa sinensis* flower extract, but as far as we are aware, there isn't much data available on the optimization and synthesis of AgNPs using the leaf extract of this plant. Plant phytochemicals were discovered to be conjugated with AgNPs by FTIR spectroscopy, which was critical in reducing and stabilizing the phytochemicals. The significant antioxidant capacity of green-synthesized NPs is indicated by their 86.23% DPPH scavenging activity at a concentration of 150 µg/ml. When tested against MDR pathogens, the produced NPs showed a significant antibacterial response, with inhibition zones spanning from 10 to 28 mm. Accordingly, the current work deduced that future nano-antibiotics targeting multidrug resistant (MDR) pathogens can be evolved using phytochemically generated NPs, as demonstrated by the findings of the antibacterial assay.

Data availability

The data that support the findings of this study are available from the corresponding author(Dr. Pamela Singh).

Authors contribution

Sonia Tyagi - Original draft, conceptualization; Pamela Singh - Supervision, Formal analysis; Vipin Khasa - Formal analysis

Funding

This research did not receive any specific grant from funding agencies in the public, commercial, or not-for-profit sectors.

Declaration of Competing interest

The authors declare that they have no competing interests.

REFERENCES

- [1] Bayda S, Adeel M, Tuccinardi T, Cordani M, Rizzolio F. The History of Nanoscience and Nanotechnology: From Chemical-Physical Applications to Nanomedicine. *Molecules*. 2019 Dec 27;25(1):112. doi: 10.3390/molecules25010112. PMID: 31892180; PMCID: PMC6982820.
- [2] Yu DG. Formation of colloidal silver nanoparticles stabilized by Na⁺-poly(gamma-glutamic acid)-silver nitrate complex via chemical reduction process. *Colloids Surf B Biointerfaces*. 2007 Oct 1;59(2):171-8. doi: 10.1016/j.colsurfb.2007.05.007. Epub 2007 May 18. PMID: 17583483.
- [3] Liu, Y. C., & Lin, L. H. (2004). New pathway for the synthesis of ultrafine silver nanoparticles from bulk silver substrates in aqueous solutions by sonoelectrochemical methods. *Electrochemistry communications*, 6(11), 1163-1168.
- [4] Mallick, K., Witcomb, M. J., & Scurrell, M. S. (2004). Polymer stabilized silver nanoparticles: a photochemical synthesis route. *Journal of materials science*, 39, 4459-4463.
- [5] Sivalingam P, Antony JJ, Siva D, Achiraman S, Anbarasu K. Mangrove Streptomyces sp. BDUKAS10 as nanofactory for fabrication of bactericidal silver nanoparticles. *Colloids Surf B Biointerfaces*. 2012 Oct 1;98:12-7. doi: 10.1016/j.colsurfb.2012.03.032. Epub 2012 Apr 28. PMID: 22652354.
- [6] Nandhakumar, E., Priya, P., Rajeswari, R., Aravindhan, V., Sasikumar, A., & Senthilkumar, N. (2019). Studies on structural, optical and thermal properties of Fe₃O₄ (NR)/ZrO₂ CSNCs synthesized via green approach for photodegradation of dyes. *Research on Chemical Intermediates*, 45, 2657-2671.

[7] Jayapriya, M., Dhanasekaran, D., Arulmozhi, M., Nandhakumar, E., Senthilkumar, N., & Sureshkumar, K. (2019). Green synthesis of silver nanoparticles using *Piper longum* catkin extract irradiated by sunlight: antibacterial and catalytic activity. *Research on Chemical Intermediates*, 45, 3617-3631.

[8] Ganapathy, M., Senthilkumar, N., Vimalan, M., Jeysekaran, R., & Potheher, I. V. (2018). Studies on optical and electrical properties of green synthesized $\text{TiO}_2@ \text{Ag}$ core-shell nanocomposite material. *Materials Research Express*, 5(4), 045020.

[9] Senthilkumar, N., Aravindhan, V., Ruckmani, K., & Potheher, I. V. (2018). *Coriandrum sativum* mediated synthesis of silver nanoparticles and evaluation of their biological characteristics. *Materials Research Express*, 5(5), 055032.

[10] N. Senthilkumar, E. Nandhakumar, P. Priya, D. Soni, M. Vimalan, I.V. Potheher, Synthesis of ZnO nanoparticles using leaf extract of *Tectona grandis* (L.) and their anti-bacterial, anti-arthritis, anti-oxidant and in vitro cytotoxicity activities, *New J. Chem.* 41 (2017) 10347–10356.

[11] Singhal, G., Bhavesh, R., Kasariya, K., Sharma, A. R., & Singh, R. P. (2011). Biosynthesis of silver nanoparticles using *Ocimum sanctum* (Tulsi) leaf extract and screening its antimicrobial activity. *Journal of nanoparticle Research*, 13, 2981-2988.

[12] Javed, B., Nadhman, A., & Razzaq, A. (2020). One-pot phytosynthesis of nano-silver from *Mentha longifolia* L.: their characterization and evaluation of photodynamic potential. *Materials Research Express*, 7(5), 055401.

[13] Kędziora A, Speruda M, Krzyżewska E, Rybka J, Łukowiak A, Bugla-Płoskońska G. Similarities and Differences between Silver Ions and Silver in Nanoforms as Antibacterial Agents. *Int J Mol Sci.* 2018 Feb 2;19(2):444. doi: 10.3390/ijms19020444. PMID: 29393866; PMCID: PMC5855666.

[14] Marchioni, M., Jounneau, P. H., Chevallet, M., Michaud-Soret, I., & Deniaud, A. (2018). Silver nanoparticle fate in mammals: Bridging in vitro and in vivo studies. *Coordination Chemistry Reviews*, 364, 118-136.

[15] Dung, T. T. N., Nam, V. N., Nhan, T. T., Ngoc, T. T. B., Minh, L. Q., Nga, B. T. T., & Quang, D. V. (2020). Silver nanoparticles as potential antiviral agents against African swine fever virus. *Materials Research Express*, 6(12), 1250g9.

[16] Erol, K., Bolat, M., Tatar, D., Nigiz, C., & Köse, D. A. (2020). Synthesis, characterization and antibacterial application of silver nanoparticle embedded composite cryogels. *Journal of Molecular Structure*, 1200, 127060.

[17] John MS, Nagoth JA, Ramasamy KP, Mancini A, Giuli G, Natalello A, Ballarini P, Miceli C, Pucciarelli S. Synthesis of Bioactive Silver Nanoparticles by a *Pseudomonas* Strain Associated with the Antarctic Psychrophilic Protozoon *Euplotes focialii*. *Mar Drugs.* 2020 Jan 3;18(1):38. doi: 10.3390/md18010038. PMID: 31947807; PMCID: PMC7024347.

[18] Hamouda RA, Hussein MH, Abo-Elmagd RA, Bawazir SS. Synthesis and biological characterization of silver nanoparticles derived from the cyanobacterium *Oscillatoria limnetica*. *Sci Rep.* 2019 Sep 10;9(1):13071. doi: 10.1038/s41598-019-49444-y. PMID: 31506473; PMCID: PMC6736842.

[19] Balraj, B., Senthilkumar, N., Potheher, I. V., & Arulmozhi, M. (2018). Characterization, antibacterial, anti-arthritis and in-vitro cytotoxic potentials of biosynthesized magnesium oxide nanomaterial. *Materials Science and Engineering: B*, 231, 121-127.

[20] Zachar, O. (2020). Formulations for COVID-19 early stage treatment via silver nanoparticles inhalation delivery at home and hospital. *ScienceOpen Preprints*.

[21] Huang, L., Sun, Y., Mahmud, S., & Liu, H. (2020a). Biological and environmental applications of silver nanoparticles synthesized using the aqueous extract of *Ginkgo biloba* leaf. *Journal of Inorganic and Organometallic Polymers and Materials*, 30, 1653-1668.

[22] Devagi P, Suresh TC, Sandhiya RV, Sairandhry M, Bharathi S, Velmurugan P, Radhakrishnan M, Sathiamoorthi T, Suresh G. Actinobacterial-Mediated Fabrication of Silver Nanoparticles and Their Broad Spectrum Antibacterial Activity Against Clinical Pathogens. *J Nanosci Nanotechnol.* 2020 May 1;20(5):2902-2910. doi: 10.1166/jnn.2020.17440. PMID: 31635627.

[23] P. Khandel, S.K. Shahi, D.K. Soni, R.K. Yadaw, L. Kanwar, *Alpinia calcarata*: potential

[24] source for the fabrication of bioactive silver nanoparticles, *Nano Convergence* 5 (2018) 37.

[25] Rajput, D., Paul, S., & Gupta, A. (2020). Green synthesis of silver nanoparticles using waste tea Leaves. *Advanced Nano Research*, 3(1), 1-14.

[26] Hemlata, Meena PR, Singh AP, Tejavath KK. Biosynthesis of Silver Nanoparticles Using *Cucumis prophetarum* Aqueous Leaf Extract and Their Antibacterial and Antiproliferative Activity Against Cancer

Cell Lines. ACS Omega. 2020 Mar 2;5(10):5520-5528. doi: 10.1021/acsomega.0c00155. PMID: 32201844; PMCID: PMC7081640.

[27] Ahmed, S., Ahmad, M., Swami, B. L., & Ikram, S. (2016). Green synthesis of silver nanoparticles using *Azadirachta indica* aqueous leaf extract. *Journal of radiation research and applied sciences*, 9(1), 1-7.

[28] Zuas, O., Hamim, N., & Sampora, Y. (2014). Bio-synthesis of silver nanoparticles using water extract of *Myrmecodia pendan* (Sarang Semut plant). *Materials Letters*, 123, 156-159.

[29] Hazarika, D., Phukan, A., Saikia, E., & Chetia, B. (2014). Phytochemical screening and synthesis of silver nanoparticles using leaf extract of *Rhynchosciadium ellipticum*. *Int J Pharm Pharm Sci*, 6(1), 672-674.

[30] Tyagi, S. (2016). Role of phytochemicals on biosynthesis of silver nanoparticles from plant extracts and their concentration dependent toxicity impacts on *Drosophila melanogaster*. *Biological Insights*, 1, 21-28.

[31] Shivananda Nayak B, Sivachandra Raju S, Orette FA, Chalapathi Rao AV. Effects of *Hibiscus rosa sinensis* L (Malvaceae) on wound healing activity: a preclinical study in a Sprague Dawley rat. *Int J Low Extrem Wounds*. 2007 Jun;6(2):76-81. doi: 10.1177/1534734607302840. PMID: 17558005.

[32] Anandan, M., Poorani, G., Boomi, P., Varunkumar, K., Anand, K., Chuturgoon, A. A., ... & Prabu, H. G. (2019). Green synthesis of anisotropic silver nanoparticles from the aqueous leaf extract of *Dodonaea viscosa* with their antibacterial and anticancer activities. *Process Biochemistry*, 80, 80-88.

[33] Sharma, N. K., Vishwakarma, J., Rai, S., Alomar, T. S., AlMasoud, N., & Bhattacharai, A. (2022). Green route synthesis and characterization techniques of silver nanoparticles and their biological adeptness. *ACS omega*, 7(31), 27004-27020.

[34] Ibrahim, S., Ahmad, Z., Manzoor, M. Z., Mujahid, M., Faheem, Z., & Adnan, A. (2021). Optimization for biogenic microbial synthesis of silver nanoparticles through response surface methodology, characterization, their antimicrobial, antioxidant, and catalytic potential. *Scientific Reports*, 11(1), 770.

[35] Tyagi, S., Singh, P., & Khasa, V. (2024). Green fabrication of silver nanoparticles with *Syzygium aromaticum* leaf extract: Characterization and applications as a biocontrol agent for multidrug resistant pathogens. *Chemical Physics Letters*, 855, 141560.

[36] Sidhu, P. K., & Nehra, K. (2021). Purification and characterization of bacteriocin Bac23 extracted from *Lactobacillus plantarum* PKLP5 and its interaction with silver nanoparticles for enhanced antimicrobial spectrum against food-borne pathogens. *Lwt*, 139, 110546.

[37] Roy A, Bulut O, Some S, Mandal AK, Yilmaz MD. Green synthesis of silver nanoparticles: biomolecule-nanoparticle organizations targeting antimicrobial activity. *RSC Adv*. 2019 Jan 21;9(5):2673-2702. doi: 10.1039/c8ra08982e. PMID: 35520490; PMCID: PMC9059941.

[38] Venkatesan, B., Subramanian, V., Tumala, A., & Vellaichamy, E. (2014). Rapid synthesis of biocompatible silver nanoparticles using aqueous extract of *Rosa damascena* petals and evaluation of their anticancer activity. *Asian Pacific journal of tropical medicine*, 7, S294-S300.

[39] Singh A, Gautam PK, Verma A, Singh V, Shivapriya PM, Shivalkar S, Sahoo AK, Samanta SK. Green synthesis of metallic nanoparticles as effective alternatives to treat antibiotics resistant bacterial infections: A review. *Biotechnol Rep (Amst)*. 2020 Jan 31;25:e00427. doi: 10.1016/j.btre.2020.e00427. Erratum in: *Biotechnol Rep (Amst)*. 2021 Mar 19;29:e00578. doi: 10.1016/j.btre.2020.e00578. PMID: 32055457; PMCID: PMC7005563.

[40] Pal, G., Rai, P., & Pandey, A. (2019). Green synthesis of nanoparticles: A greener approach for a cleaner future. In *Green synthesis, characterization and applications of nanoparticles* (pp. 1-26). Elsevier.

[41] Qasim Nasar, M., Zohra, T., Khalil, A. T., Saqib, S., Ayaz, M., Ahmad, A., & Shinwari, Z. K. (2019). *Seripecten quettense* mediated green synthesis of biogenic silver nanoparticles and their theranostic applications. *Green Chemistry Letters and Reviews*, 12(3), 310-322.

[42] Ansari M, Ahmed S, Abbasi A, Khan MT, Subhan M, Bukhari NA, Hatamleh AA, Abdelsalam NR. Plant mediated fabrication of silver nanoparticles, process optimization, and impact on tomato plant. *Sci Rep*. 2023 Oct 23;13(1):18048. doi: 10.1038/s41598-023-45038-x. PMID: 37872286; PMCID: PMC10593853.

[43] Aldabaan, N. A., Turakani, B., Mahnashi, M. H., Shaikh, I. A., Alhazmi, A. Y., Almasoudi, H. H., ... & Iqbal, S. S. (2024). Evaluation of antimicrobial, anticancer, antidiabetic, antioxidant activities and silver nanoparticles synthesized from Indian Clove-*Syzygium aromaticum* leaf extract. *Journal of King Saud University-Science*, 36(4), 103142.

[44] Younas, M., Rasool, M. H., Khurshid, M., Khan, A., Nawaz, M. Z., Ahmad, I., & Lakhan, M. N. (2023). *Moringa oleifera* leaf extract mediated green synthesis of silver nanoparticles and their antibacterial effect against selected gram-negative strains. *Biochemical Systematics and Ecology*, 107, 104605.

<https://doi.org/10.1016/j.bse.2023.104605>

[45] Ahsan, A., Farooq, M. A., Ahsan Bajwa, A., & Parveen, A. (2020). Green synthesis of silver nanoparticles using *Parthenium hysterophorus*: optimization, characterization and in vitro therapeutic evaluation. *Molecules*, 25(15), 3324.

[46] Jalab, J., Abdelwahed, W., Kitaz, A., & Al-Kayali, R. (2021). Green synthesis of silver nanoparticles using aqueous extract of *Acacia cyanophylla* and its antibacterial activity. *Heliyon*, 7(9).

[47] Anigol, L. B., Charantimath, J. S., & Gurubasavaraj, P. M. (2017). Effect of concentration and pH on the size of silver nanoparticles synthesized by green chemistry. *Org. Med. Chem. Int. J.*, 3(5), 1-5.

[48] Elemike, E. E., Onwudiwe, D. C., Ogeleka, D. F., & Mbonu, J. I. (2019). Phyto-assisted preparation of Ag and Ag–CuO nanoparticles using aqueous extracts of *Mimosa pigra* and their catalytic activities in the degradation of some common pollutants. *Journal of Inorganic and Organometallic Polymers and Materials*, 29, 1798-1806.

[49] Huang, W., Yan, M., Duan, H., Bi, Y., Cheng, X., & Yu, H. (2020b). Synergistic antifungal activity of green synthesized silver nanoparticles and epoxiconazole against *Setosphaeria turcica*. *Journal of Nanomaterials*, 2020(1), 9535432.

[50] Madivoli, E. S., Kareru, P. G., Gachanja, A. N., Mugo, S. M., Makhanu, D. S., Wanakai, S. I., & Gavamukulya, Y. (2020). Facile synthesis of silver nanoparticles using *Lantana trifolia* aqueous extracts and their antibacterial activity. *Journal of Inorganic and Organometallic Polymers and Materials*, 30(8), 2842-2850.

[51] Ngoepe, N. M., Mbita, Z., Mathipa, M., Mketu, N., Ntsendwana, B., & Hintsho-Mbita, N. C. (2018). Biogenic synthesis of ZnO nanoparticles using *Monsonia burkeana* for use in photocatalytic, antibacterial and anticancer applications. *Ceramics International*, 44(14), 16999-17006. <https://doi.org/10.1016/j.ceramint.2018.06.142>

[52] Qais, F. A., Shafiq, A., Khan, H. M., Husain, F. M., Khan, R. A., Alenazi, B., Alsalme, A., & Ahmad, I. (2019). Antibacterial Effect of Silver Nanoparticles Synthesized Using *Murraya koenigii* (L.) against Multidrug-Resistant Pathogens. *Bioinorganic chemistry and applications*, 2019, 4649506. <https://doi.org/10.1155/2019/4649506>

[53] Mani, M., Pavithra, S., Mohanraj, K., Kumaresan, S., Alotaibi, S. S., Eraqi, M. M., Gandhi, A. D., Babajanarthanam, R., Maaza, M., & Kaviyarasu, K. (2021). Studies on the spectrometric analysis of metallic silver nanoparticles (Ag NPs) using *Basella alba* leaf for the antibacterial activities. *Environmental research*, 199, 111274. <https://doi.org/10.1016/j.envres.2021.111274>

[54] Chand, K., Cao, D., Fouad, D. E., Shah, A. H., Dayo, A. Q., Zhu, K., ... & Dong, S. (2020). Green synthesis, characterization and photocatalytic application of silver nanoparticles synthesized by various plant extracts. *Arabian Journal of Chemistry*, 13(11), 8248-8261. <https://doi.org/10.1016/j.arabjc.2020.01.009>

[55] Oda AM, Abdulkadhim H, Jabuk SIA, Hashim R, Fadhil I, Alaa D, Kareem A. Green synthesis of silver nanoparticle by cauliflower extract: characterisation and antibacterial activity against storage. *IET Nanobiotechnol*. 2019 Apr 17;13(5):530–5. doi: 10.1049/iet-nbt.2018.5095. PMID: PMC8676221.

[56] Shah, S., Gaikwad, S., Nagar, S., Kulshrestha, S., Vaidya, V., Nawani, N., & Pawar, S. (2019). Biofilm inhibition and anti-quorum sensing activity of phytosynthesized silver nanoparticles against the nosocomial pathogen *Pseudomonas aeruginosa*. *Biofouling*, 35(1), 34–49. <https://doi.org/10.1080/08927014.2018.1563686>

[57] Jamdagni, P., Khatri, P., & Rana, J. S. (2018). Biogenic synthesis of silver nanoparticles from leaf extract of *Elettaria cardamomum* and their antifungal activity against phytopathogens. *Advanced Materials Proceedings*, 3(3), 129-135. DOI: 10.5185/amp.2018/977

[58] Sidhu, P. K., & Nehra, K. (2021). Purification and characterization of bacteriocin Bac23 extracted from *Lactobacillus plantarum* PKLP5 and its interaction with silver nanoparticles for enhanced antimicrobial spectrum against food-borne pathogens. *Lwt*, 139, 110546.

[59] Khan FU, Chen Y, Khan NU, Khan ZU, Khan AU, Ahmad A, Tahir K, Wang L, Khan MR, Wan P. Antioxidant and catalytic applications of silver nanoparticles using *Dimocarpus longan* seed extract as a reducing and stabilizing agent. *J Photochem Photobiol B*. 2016 Nov;164:344-351. doi: 10.1016/j.jphotobiol.2016.09.042. Epub 2016 Oct 3. PMID: 27723492.

[60] Bruna T, Maldonado-Bravo F, Jara P, Caro N. Silver Nanoparticles and Their Antibacterial Applications. *Int J Mol Sci*. 2021 Jul 4;22(13):7202. doi: 10.3390/ijms22137202. PMID: 34281254; PMCID: PMC8268496.